Dynamic-Quantizer-Based Periodic Event-Triggered Control of Nonlinear Systems: Quantization After or Before Sampling

***Abstract*—This paper investigates the event-triggered quantized control for nonlinear systems with external disturbances by exploiting both temporal and spatial aspects. In order to cope with the issues that inhibit the practical implementation such as the continuous monitoring of the event-triggering condition and finite-bit data at each transmission, the periodic event-triggering mechanism and the dynamic quantizer are employed respectively. Two configurations of the event-based quantized controller, i.e., quantization after sampling and quantization before sampling, are discussed for the wider utilization of the quantized control. By exploiting the hybrid system approach, the resulting control systems in the two configurations can be modeled and guaranteed to possess input-to-state stability property of a size-adjustable set around the origin. With a joint design of the event-triggering mechanism, the dynamic quantizer and the sampling period, the performance of the closed-loop system can be regulated by a trade-off between transmission and quantization without Zeno behavior. The effectiveness of the proposed approach is illustrated in numerical examples.**

I. Introduction

In the last two decades, networked control systems (NCS) have received considerable attention due to its widespread applications in paramount areas [1], [2]. In NCS, the sensors, the controllers, and the actuators communicate and interact with each other over network communication channels. Compared with traditional wired control systems, these systems have several advantages including increased flexibility, lower cost and ease of maintenance. However, limited resources of wireless communication, namely *limited transmission energy* and *limited transmission bandwidth*, bring new challenges in NCS. For one thing, the traditional sampled-data control adopted in most existing works, which executes transmission every fixed time unit, is sometimes a waste usage of communication energy. In order to tackle this drawback, event-triggered control (ETC) approaches have been introduced and proved to be an efficient way to reduce communication burden [3]–[5]. For another, limited transmission data rate is a common constraint in digital network systems, while most studies consider the ideal case that the transmitted information is exactly accurate. To this end, an appropriate quantization mechanism is required to cope with this constraint, which promotes the quantized control [6], [7].

In ETC schemes, the transmission actions are carried out only when a certain well-designed triggering condition is satisfied. In this sense, unnecessary transmissions when the transmitted data is not vital for the stability or performance of the system can be prevented. Most works on ETC focus on the continuous event-triggered control (CETC), see, e.g. [8]–[10], which means the evaluation of triggering conditions is carried out at all times. It can be known that such a continuous evaluation of the event conditions may result in great computation cost, and even is not possible for digital implementations. To overcome this problem, periodic event-triggered control (PETC) was proposed [11]–[15]. It inherits the benefits of sampled-data control and event-triggered control, in the sense that the triggering condition is only evaluated periodically at the predefined discrete time sequence. Moreover, Zeno-behavior, i.e., the appearance of infinite numbers of transmissions in finite time, is naturally excluded in PETC.

Due to the limited communication bandwidth in NCS, another accompanying issue, that the transmitted information at each transmission instant can not be exactly accurate, is also required to be carefully handled. The information should be processed through a quantization mechanism into finite bits before each transmission. Significant contributions have been made to deal with the stability problems in the presence of quantization-induced errors [16]–[26]. To mention a few, a sector-bounded approach in [16] is utilized to stabilize the linear system with quantization. In order to improve the control performance and avoid the quantization saturation phenomenon with limited quantization regions, the work in [17] presented a dynamic quantizer, of which the quantizer range and sensitivity keep varying according to the actual state. The authors in [18] combined the information theory and the control theory to exponentially stabilize the linear system with finite data and bounded bit rates. Output-based event-triggered control of linear systems with dynamic quantization was investigated in [19], [20]. It should be mentioned that most quantized control methods focus on linear systems, with a few exceptions, see [21], [22]. In [22], a dynamic quantization mechanism of which the quantization variable is based on a differential equation, was proposed to guarantee the input-to-state stability. However, few techniques are developed to the partial state feedback control and the quantized control with external disturbances existing for nonlinear systems. Apparently, quantized control for nonlinear systems with disturbances is at its early stage and deserves much more research attention.

Nowadays, event-based quantized control has attracted considerable attention due to its superiority of efficient use of communication resources in digital systems. However, it should be noted that the guarantee of the practical implementation in event-triggered quantized control is not a trivial thing, since the introduction of quantization also brings some challenges such as the avoidance of accumulation of quantization events, finite data bits at each transmission and the resistance to external disturbances, see [7], [20] for more discussions. Moreover, as mentioned in [20], [22], it might

be the cases in some practical scenarios that the quantization process is before the event-triggering sampling. To the best of our knowledge, only the works in [22], [24] investigate the case of quantization before sampling with the assumption of no disturbances. In addition, continuous evaluation of the event-triggering condition, as we mentioned before, also obstructs the way for digital implementation. Hence, the periodic event-triggered quantized control (PETQC), as a possible alternative to counter these drawbacks, is naturally of interest. Despite its importance to pave the way for digital implementation, as far as we know, only the authors in [23] investigated periodic event-triggered control problem with quantization, based on a linear matrix inequality (LMI) approach. Therefore, more attention is deserved for this largely under-explored domain. In particular, there is a need for systematic methods, which are capable of handling nonlinear systems, output feedback and external disturbances.

Motivated by the above observations, in this paper, the quantized control for nonlinear systems with the periodic event-triggering mechanism sampling is investigated. Specially, we consider two configurations of the periodic event-triggered quantized control: quantization after sampling (S-Q) and quantization before sampling (Q-S). For both cases, we present a systematic method to jointly design the dynamic quantizer, the event-triggering mechanism and the sampling period. Due to the periodic mechanism, phenomena including the Zeno behavior in transmission and accumulation of zoom actions of the dynamic quantizer are prevented. The quantizer saturation in the quantization process is also avoided by using the adaptive quantization strategy. The main contributions of this work can be summarized as follows:

1. A systematic approach is proposed to address the output-based periodic event-triggered control problem for nonlinear systems with the quantization effect. In our method, by virtue of a new kind of hybrid Lyapunov function, the ISS property is guaranteed for a bounded set around the origin with respect to the external disturbances, whose size can be made arbitrarily small by appropriately selecting the parameters.
2. Both the quantization after sampling and quantization before sampling cases are considered. For both two cases, the forms of the event-triggering conditions, dynamic quantizers as well as the rules on selecting sampling period, are provided explicitly. In both two cases, the desired ISS property can be achieved.

The rest of the paper is organized as follows. The preliminaries and problem formulation are presented in section II. The main results for the S-Q case and Q-S case are given in Section III and Section IV, respectively. Simulation results are provided in Section V and the conclusion is drawn in Section VI.

Notations: The set of real numbers is denoted by $\mathbb{R}$ and the set of non-negative real integers is denoted by $\mathbb{R}_{\geq 0}$. For vectors v_1, v_2, ..., $v_n \in \mathbb{R}^n$, we denote the vector $[v_1^T, v_2^T, ..., v_n^T]^T$ by $(v_1, v_2, ...v_n)$. We write I_n to state the identity matrix of dimension n. For a symmetric matrix A, $\lambda_{\max}(A)$ and $\lambda_{\min}(A)$ denote the maximum and minimum eigenvalues of A, respectively. For a vector x, we denote by $|x| := \sqrt{x^T x}$ its Euclidean norm and, for a matrix A, $|A| := \sqrt{\lambda_{\max}(A^T A)}$. Given a set $\mathcal{A} \subseteq \mathbb{R}^n$ and $x \in \mathbb{R}^n$, we define the distance of x to $\mathcal{A}$ as $|x|_{\mathcal{A}} := \inf_{y \in \mathcal{A}} |x - y|$. A function α: $\mathbb{R}_{\geq 0} \to \mathbb{R}_{\geq 0}$ is said to be of class $\mathcal{K}$ if it is continuous, strictly increasing and $\alpha(0) = 0$. It is said to be class $\mathcal{K}_\infty$ if in addition it is unbounded. A continuous function β: $\mathbb{R}_{\geq 0} \times \mathbb{R}_{\geq 0} \to \mathbb{R}_{\geq 0}$ is said to be of class $\mathcal{KL}$ if, for each $t \in \mathbb{R}_{\geq 0}$, $\beta(\cdot, t)$ is of class $\mathcal{K}$, and for each $s \in \mathbb{R}_{\geq 0}$, $\beta(s, \cdot)$ is decreasing to 0. A continuous function $\gamma : \mathbb{R}_{\geq} 0 \times \mathbb{R}_{\geq} 0 \times \mathbb{R}_{\geq} 0 \to \mathbb{R}_{\geq} 0$ is said to be class $\mathcal{KLL}$ if, for each $r \in \mathbb{R}_{\geq 0}$, both $\gamma(\cdot, r, \cdot)$ and $\gamma(\cdot, \cdot, r)$ belong to class $\mathcal{KL}$. By $\langle \cdot, \cdot \rangle$, we denote the usual inner product of real vectors. For x, $v \in \mathbb{R}$, and locally Lipschitz $U : \mathbb{R}^n \to \mathbb{R}$, $U^\circ(x; v)$ is the Clark derivative of the function U at x in the direction v, i.e., $U^\circ(x; v) := \limsup_{y \to x, \lambda \downarrow 0} \frac{U(y+\lambda v) - U(y)}{\lambda}$.

II. Preliminaries and Problem Formulation

A. Plant and Controller

Consider the following nonlinear system as the plant represented by:

$$\dot{x}_p = f_p(x_p, u, w), \quad y = g_p(x_p) \tag{1}$$

where $x_p \in \mathbb{R}^{n_p}$ denotes the system state, $w \in \mathbb{R}^{n_w}$ is the system disturbance, and $y \in \mathbb{R}^{n_y}$ is the system measurement output. $u \in \mathbb{R}^{n_u}$ is the control input, which is generated by a dynamic controller of the following form:

$$\dot{x}_c = f_c(x_c, y), \quad u = g_c(x_c, y) \tag{2}$$

where $x_c \in \mathbb{R}^{n_c}$ denotes the controller state. The functions f_p and f_c are assumed to be continuous and the functions g_p and g_c are assumed to be continuously differentiable. The controller (2) is designed using the emulation-based approach [27], of which the closed-loop system is stable without the quantization effect and network setup.

B. Dynamic Quantizer

As we all know, the output of a quantizer is a piecewise constant. Define the piecewise constant function $q : \mathbb{R}^{n_z} \to \mathbb{Q}$, where $\mathbb{Q}$ is a finite subset of $\mathbb{R}^{n_z}$. We assume that the function q satisfies the following assumption.

Assumption 1: [21] There exist constants M and Δ such that for all $z \in \mathbb{R}^{n_z}$, it holds that

$$|z| \leq M \Rightarrow |q(z) - z| \leq \Delta. \tag{3}$$

Moreover, there exist a constant $\sigma > 0$ such that for all $l \in \mathbb{R}^{n_z}$ with $|l| \leq \sigma$, it holds that $q(l) = 0$.

In this paper, we implement the following dynamic quantizer:

$$q_\mu(z) = \mu q(\frac{z}{\mu}) \tag{4}$$

where μ is the zoom variable and the function q satisfies Assumption 1 for some M, Δ. The zoom variable is varied based on the true value of measurement and aims to adjust the quantizer range such that limited data bits can be efficiently used. For each fixed μ, the range of the dynamic quantizer

is $M\mu$, and the error bound is $\Delta\mu$. In order to transmit data effectively and avoid the saturation phenomenon at the same time, suitable zoom actions should be taken before each transmission. We use the zoom update strategy which is defined as

$$\mu^+ \in \Theta(y,\mu) := \Omega_{\text{in}}^{\kappa_{\text{in}}(y,\mu)}\Omega_{\text{out}}^{\kappa_{\text{out}}(y,\mu)}\mu \tag{5}$$

where Ω_{in} and Ω_{out} are zoom-in and zoom-out factors, respectively. The functions κ_{in}, κ_{out} decide the number of zoom-in or zoom-out actions that needs to be performed. We assume that the initial values of the quantizer variable μ of both the encoder and decoder sides are the same, and the quantization region $\mathbb{Q}$, zoom factors Ω_{in}, Ω_{out} are known at both the encoder and decoder sides. The encoder could only transmit the index of the quantization region, the number of the required zoom actions, and a boolean that illustrates whether to zoom in or zoom out. More details about the design of the dynamic quantizer will be introduced in Section III.A and Section IV.A.

C. Event-Triggering Mechanism

The event-triggering mechanism utilizes locally available information and decides the time instant of the transmission. The triggering mechanism is evaluated at each sampling instant $t_j = jh$, $j \in \mathbb{N}$, where

$$h_0 \leq h \leq \mathcal{T} \tag{6}$$

with $\mathcal{T} > 0$ the upper bound on the inter-sampling time and h_0 the minimum time between two transmission induced by practical hardware constraints. The transmission sequence is a subsequence of the sampling sequence and thus the Zeno-behavior is naturally avoided due to the periodic implementation. We denote the transmission sequences of S-Q and Q-S cases as $\{t_k^{SQ}\}$ and $\{t_k^{QS}\}$, with $k \in \mathbb{N}$.

The event-triggering mechanisms of S-Q and Q-S cases are as follows:

$$t_{k+1}^{SQ} = \min_{j\in\mathbb{Z}_{\geq 0}} \{jh | jh > t_k^{SQ},\ \Upsilon^{SQ}(o^{SQ}) \geq 0), \tag{7}$$

$$t_{k+1}^{QS} = \min_{j\in\mathbb{Z}_{\geq 0}} \{jh | jh > t_k^{QS},\ \Upsilon^{QS}(o^{QS}) \geq 0) \tag{8}$$

where o^{SQ}, o^{QS} are locally available information in two cases, and $\Upsilon^{SQ}(\cdot)$, $\Upsilon^{QS}(\cdot)$ are triggering conditions of two cases, respectively. More details will be specified in Section III.B and Section IV.B.

D. System Setup Description

Before presenting out works, let us briefly introduce how the data is processed and transmitted in the network system. We consider the scenario where the controller is co-located with the actuator, and the sensor measurement y is sampled and transmitted to the controller over a digital channel. The transmission- and computation-induced delays are ignored in this study. Both the quantization after the event-triggered sampling and quantization before sampling cases are investigated.

(1) System setup: S-Q case

In the quantization after sampling case as shown in Fig. 1, the event-triggering mechanism is periodically evaluated to determine whether or not to transmit the sampling of measurement $y(jh)$. If the predefined event is triggered at the time instant jh, the quantizer will complete the encoding and transmission of finite bits of data to the controller immediately. As a result, the most recently transmitted quantized sensor measurement, which is denoted by $\hat{y}_q$, is reset to $q_\mu(y(jh))$ at $t = jh$. Zero-order-hold (ZOH) devices are used for implementation, i.e., the value $\hat{y}_q$ is kept constant between two consecutive transmission instants.

(2) System setup: Q-S case

In the quantization before sampling case, as shown in Fig. 2, the quantization process is done at each sampling instant before the event-triggering detection of sampling. In other words, the event-triggering mechanism utilizes the quantized sampling of measurement $q_\mu(y(jh))$ to make the decision of transmission at each sampling instant. ZOH devices are also utilized.

For both cases, we assume that the quantizer has access to the true(current) sensor measurement. One of the main differences between these two cases is the locally available data in the event-triggering mechanism, as we will explain in detail later.

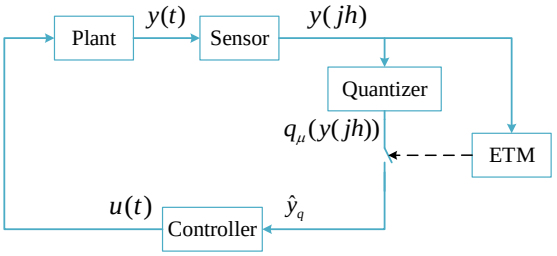

Fig. 1. The block diagram of the closed-loop NCS: S-Q case.

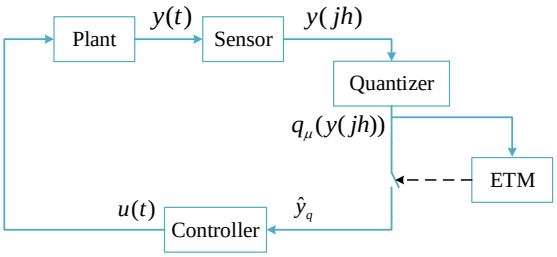

Fig. 2. The block diagram of the closed-loop NCS: Q-S case.

E. Hybrid Model Description

The hybrid system exhibits both continuous and discrete dynamic behavior and is therefore suitable for modeling the event-triggered dynamical systems. In this section, by using the hybrid system framework, the hybrid models for both the S-Q case and the Q-S case are constructed for the closed-loop system. For more details of the hybrid system including the hybrid time domain, hybrid signal and so on, we refer readers to [14], [28] and [29].

(1) Hybrid Model: S-Q Case

Before presenting the overall hybrid system, we first define the sampling-induced error $e_s(t) = \hat{y}(t) - y(t)$ with $\hat{y}(t)$ the most recently sampled measurement signal, the quantization-induced error $e_q(t) = \hat{y}_q(t) - \hat{y}(t)$ with $\hat{y}_q(t)$ the most recently transmitted quantized signal, $\hat{y}(t) = y(jh)$ for $t \in [jh, (j+1)h)$. We then define the total network-induced error as

$$e(t) = e_q(t) + e_s(t) = \hat{y}_q(t) - y(t). \tag{9}$$

Note that at each transmission instant t_k^{SQ}, $k \in \mathbb{N}$, only the sampling-induced error e_s is reset to 0, and the total error is reset to quantization-induced error

$$e\left((t_k^{SQ})^+\right) = e_q\left((t_k^{SQ})^+\right). \tag{10}$$

We also introduce a variable τ to represent the elapsed time since the last evaluation of the triggering condition, and a boolean variable p to keep track of whether at the next event, the zoom variable is updated ($p = 0$) or a transmission occurs ($p = 1$). Let $x := (x_p, x_c) \in \mathbb{R}^{n_x}$, $\xi := (x, e, \tau, \mu, p) \in \mathbb{X}$ with $\mathbb{X} = \mathbb{R}^{n_x} \times \mathbb{R}^{n_y} \times \mathbb{R}_{\geq 0} \times \mathbb{R}_{\geq 0} \times \{0, 1\}$. The flow set $\mathcal{C}$ and the jump set $\mathcal{D}$ are given by

$$\begin{aligned} \mathcal{C} &:= \{\xi \in \mathbb{X} : p = 0\} \\ \mathcal{D} &:= \{\xi \in \mathbb{X} : \tau = h\} \end{aligned} \tag{11}$$

Given (11), we obtain the hybrid model as follows.

$$\begin{aligned} \dot{\xi} &\in F(\xi, w) && \xi \in \mathcal{C} \\ \xi^+ &\in G^{SQ}(\xi) && \xi \in \mathcal{D} \end{aligned} \tag{12}$$

where ξ^+ denotes the state of ξ right after the jump, and the flow map is given by

$$F(\xi, w) = (f(x, e, w), g(x, e, w), 1, 0, 0) \tag{13}$$

with

$$\begin{aligned} f(x, e, w) &= \Big(f_p\big(x_p, g_c(x_c, e + g_p(x_p)), w\big), \\ &\qquad f_c(x_c, g_p(x_p) + e)\Big), \\ g(x, e, w) &= -\frac{\partial g_p(x_p)}{\partial x_p} f_p\big(x_p, g_c(x_c, e + g_p(x_p)), w\big). \end{aligned}$$

The jump map is given by

$$G^{SQ}(\xi) := \begin{cases} G_\mu^{SQ}(\xi), & \xi \in \mathcal{D} \wedge p = 0 \wedge \Upsilon^{SQ} \geq 0 \\ G_y^{SQ}(\xi), & \xi \in \mathcal{D} \wedge p = 1 \\ G_0^{SQ}(\xi), & \xi \in \mathcal{D} \wedge p = 0 \wedge \Upsilon^{SQ} < 0 \end{cases} \tag{14}$$

with $G_\mu^{SQ}(\xi) = (x, e, \tau, \mu^+, 1)$, $G_y^{SQ}(\xi) = (x, e_q, 0, \mu, 0)$ and $G_0^{SQ}(\xi) = (x, e, 0, \mu, 0)$, where μ^+ is updated according to (5).

Remark 1: The introduction of the boolean variable p enables us to describe the orders of which the update of the quantizer variable and the transmission happen. Except at the sampling instants, the system (12) flows on the set $\mathcal{C}$ and the variable p is set as 0. At each sampling instant, the event-triggering condition is verified to decide whether or not to transmit information and ξ will jump according to (14). If $\Upsilon^{SQ} \geq 0$ at some sampling instant, ξ will jump according to $G_\mu^{SQ}(\xi)$, which corresponds to an update of the quantizer variable μ and p is reset to 1. Since the system is not allowed to flow when $p = 1$, ξ subsequently jumps according to $G_y^{SQ}(\xi)$, and a transmission is generated with p going back to 0. If $\Upsilon^{SQ} < 0$, ξ will jump according to $G_0^{SQ}(\xi)$ and the variables remain the same except that τ is reset to 0. Such kind of modeling method is also applied in the Q-S case, as mentioned in the subsequent content.

(2) Hybrid Model: Q-S Case

For the Q-S case, we define the quantization-induced error $e_q(t) = q_\mu(y(t)) - y(t)$ with $q_\mu(y(t))$ the quantized signal, and the sampling-induced error $e_s(t) = \hat{y}_q(t) - q_\mu(y(t))$ with $\hat{y}_q(t)$ the most recently transmitted quantized signal. We then define the total network-induced error as

$$e(t) = e_q(t) + e_s(t) = \hat{y}_q(t) - y(t). \tag{15}$$

Note that the definitions of e_q and e_s are different from those in S-Q case since the orders of event-triggering evaluation and the quantization are different. At each transmission instant t_k^{QS}, $k \in \mathbb{N}$, the total error is reset to quantization-induced error

$$e\left((t_k^{QS})^+\right) = e_q\left((t_k^{QS})^+\right). \tag{16}$$

We then obtain the overall hybrid model:

$$\begin{aligned} \dot{\xi} &\in F(\xi, w) && \xi \in \mathcal{C} \\ \xi^+ &\in G^{QS}(\xi) && \xi \in \mathcal{D} \end{aligned} \tag{17}$$

where the flow and jump sets as in (11) and the flow map as in (13). The jump map is given by

$$G^{QS}(\xi) := \begin{cases} G_\mu^{QS}(\xi) & \xi \in \mathcal{D} \wedge p = 0 \\ G_y^{QS}(\xi) & \xi \in \mathcal{D} \wedge p = 1 \wedge \Upsilon^{QS} \geq 0 \\ G_0^{QS}(\xi) & \xi \in \mathcal{D} \wedge p = 1 \wedge \Upsilon^{QS} < 0 \end{cases} \tag{18}$$

with $G_\mu^{QS}(\xi) = (x, e, \tau, \mu^+, 1)$, $G_y^{SQ}(\xi) = (x, e_q, 0, \mu, 0)$, and $G_0^{SQ}(\xi) = (x, e, 0, \mu, 0)$.

At each sampling instant, the dynamic quantizer quantizes the output measurement, and then the event-triggering mechanism decides whether or not to transmit the quantized information. As shown in the jump map, the zoom variable μ jumps according to $G_\mu^{QS}(\xi)$ at each sampling instant, and the dynamic quantizer operates regardless of the event trigger, which is one of the differences from the S-Q case. Subsequently, ξ jumps according to $G_y^{QS}(\xi)$ or $G_0^{QS}(\xi)$ depending upon whether the event-triggering condition is satisfied or not.

F. Preliminaries

Below are some definitions and assumptions used in this paper.

Definition 1: For a hybrid signal w, with domain dom $w \subset \mathbb{R}_{\geq 0} \times \mathbb{N}$, and a scalar $T \in \mathbb{R}_{\geq 0}$, the T-truncated $\mathcal{L}_\infty$-norm is given by

$$||w_{[T]}||_\infty := \sup_{j \in \mathbb{N}} \left\{ \operatorname*{ess\,sup}_{t \in \mathbb{R}_{\geq 0} | (t,j) \in \text{dom } w, t+j \leq T} |w(t, j)| \right\}. \tag{19}$$

The $\mathcal{L}_\infty$-norm of w is given by

$$||w||_\infty := \lim_{T \to T^*} ||w_{[T]}||_\infty \tag{20}$$

where $T^* := \sup\{t + j : (t, j) \in \text{dom } w\}$. We say that $w \in \mathcal{L}_\infty$ whenever the above limit exists and is finite.

Definition 2: Consider the hybrid systems (12) or (17), a set $\mathcal{A} \subset \mathbb{R}^{n_x}$ and a set $\mathbb{X}_0 \subseteq \mathbb{R}^{n_x}$. The set $\mathcal{A}$ is ISS w.r.t. w and initial state set $\mathbb{X}_0$ if there exist $\beta \in \mathcal{KL}$ and $\psi \in \mathcal{K}$ such that, for each $x(0,0) \in \mathbb{X}_0$ and $w \in \mathcal{L}_\infty$, each maximal solution pair (x, w) is t-complete and satisfies for all $(t, j) \in \mathrm{dom}\, x$,

$$|x(t,j)|_{\mathcal{A}} \leq \max\{\beta(|x(0,0)|_{\mathcal{A}}, t+j), \psi(||w||_\infty)\}. \quad (21)$$

Assumption 2: There exist a locally Lipschitz function $W(e) : \mathbb{R}^{n_y} \to \mathbb{R}_{\geq 0}$ with W positive definite, a continuous function $H(x, e, w) : \mathbb{R}^{n_x} \times \mathbb{R}^{n_y} \times \mathbb{R}^{n_w} \to \mathbb{R}_{\geq 0}$, and the constants $\underline{\alpha}_W$, $\overline{\alpha}_W$, $L_W > 0$ such that

(i) For all $e \in \mathbb{R}^{n_e}$, $\underline{\alpha}_W|e| \leq W(e) \leq \overline{\alpha}_W|e|$

(ii) For almost all $e \in \mathbb{R}^{n_y}$, and all $(x, w) \in \mathbb{R}^{n_x} \times \mathbb{R}^{n_w}$, $\left\langle \frac{\partial W}{\partial e}, g(x, e, w) \right\rangle \leq L_W W(e) + H(x, e, w)$

Assumption 3: There exist a locally Lipschitz function $V : \mathbb{R}^{n_x} \to \mathbb{R}_{\geq 0}$, $\underline{\alpha}_V$, $\overline{\alpha}_V \in \mathcal{K}_\infty$, a locally Lipschitz function $J(x, e, w) : \mathbb{R}^{n_x} \times \mathbb{R}^{n_y} \times \mathbb{R}^{n_w} \to \mathbb{R}_{\geq 0}$, constants α_V, σ_V, ε_y, $\gamma > 0$ and $L_{\varepsilon_y} \in (0, 1]$, such that

(i) For all $x \in \mathbb{R}^{n_x}$, $\underline{\alpha}_V(|x|) \leq V(x) \leq \overline{\alpha}_V(|x|)$

(ii) For almost all $x \in \mathbb{R}^{n_x}$ and all $(e, w) \in \mathbb{R}^{n_y} \times \mathbb{R}^{n_w}$, $\langle \nabla V(x), f(x, e, w) \rangle \leq -\alpha_V|x|^2 + \sigma_V|w|^2 + \gamma^2 W^2(e) - \varepsilon_y|y|^2 - H^2(x, e, w) - J(x, e, w)$

(iii) For almost all $x \in \mathbb{R}^{n_x}$ and all $(e, w) \in \mathbb{R}^{n_y} \times \mathbb{R}^{n_w}$, $\left\langle \nabla \varepsilon_y|y|^2, -g(x, e, w) \right\rangle \leq L_{\varepsilon_y}\varepsilon_y|y|^2 + H^2(x, e, w) + J(x, e, w)$

The Assumptions 2-3 are the same in essence as the assumptions in [13], [14], which are applicable in many kinds of nonlinear systems. The item (ii) of Assumption 3 indicates that the origin is ISS with respect to input (e, w) without quantization. Item (iii) of Assumption 3 implies $|y|^2$ has an exponential growth condition on flows, where the function $J(x, e, w)$ is used to collect the redundant terms.

G. Problem Statement

Our objective is to achieve the stability property of the closed-loop system for both the S-Q and the Q-S cases. Specifically, we aim to jointly design the event-triggering mechanisms, the dynamic quantizers and the sampling period such that the ISS property is guaranteed for the considered nonlinear systems with disturbances.

III. Main Results: Quantization After Sampling (S-Q) Case

In this section, we first focus on the S-Q case for the parameter design of the quantizer and the event-triggering mechanism, which is mathematically simpler. The stability of the resulting closed-loop system is analyzed.

A. Design of the Dynamic Quantizer

When designing the dynamic quantizer, we intend to make sure that the output measurement is well-displayed with finite bits such that the quantization error is small as much as possible and the saturation phenomenon is avoided. In terms of the dynamic quantization mechanism in (4)-(5), our assignment is to design the initial quantizer range M, the initial error bound Δ, the zoom-in scale parameter $\Omega_{\mathrm{in}} \in (0, 1)$, the zoom-out scale parameter $\Omega_{\mathrm{out}} > 1$, the zoom-in range parameters ℓ_{in}, and the zoom-out range parameter ℓ_{out}. In order to keep the measurement staying within a suitable quantization region, the quantization strategy is implemented as follows [20]:

$$\begin{aligned}
&\mu^+ := \Omega_{\mathrm{in}}^{\kappa_{\mathrm{in}}(y(jh),\mu)}\Omega_{\mathrm{out}}^{\kappa_{\mathrm{out}}(y(jh),\mu)}\mu \\
&\kappa_{\mathrm{in}}(y(jh),\mu) \\
&= \left\lceil \max\left\{-\zeta, \frac{\log\left(\max\left\{|y(jh)|, \Delta_0\right\}/(\ell_{\mathrm{in}}\mu)\right)}{\log \Omega_{\mathrm{in}}}\right\}\right\rceil \\
&\kappa_{\mathrm{out}}(y(jh),\mu) = \left\lceil \max\left\{-\zeta, \frac{\log\left(|y(jh)|/\ell_{\mathrm{out}}\mu\right)}{\log \Omega_{\mathrm{out}}}\right\}\right\rceil \quad (22)
\end{aligned}$$

where

$$\ell_{\mathrm{in}} = \Omega_{\mathrm{in}}(M - \kappa\Delta), \quad \ell_{\mathrm{out}} = M - \Delta \quad (23)$$

with

$$\kappa > \max\left\{1, \frac{(\Omega_{\mathrm{in}}\Omega_{\mathrm{out}} - 1)M + \Delta}{\Omega_{\mathrm{in}}\Omega_{\mathrm{out}}\Delta}\right\} \quad (24)$$

and where the constant $\zeta \in (0, 1)$ can be arbitrarily chosen.

Moreover, the number of quantization regions required for stability satisfies

$$\frac{M}{\Delta} \geq \kappa + \frac{\overline{\alpha}_W\sqrt{\gamma}}{\Omega_{\mathrm{in}}\sqrt{\pi\rho^3(\pi)\varepsilon_y}} \quad (25)$$

with γ, ε_y, $\overline{\alpha}_W$ as mentioned in Assumption 2 and 3, and π, $\rho(\pi)$ being parameters in the event-triggering mechanism and will be specified in Section III.B. Note that (25) provides a lower bound on the number of the quantization regions, i.e., the quantizer accuracy is required to reach a certain degree to not destroy the stability property.

B. Design of the Event-triggering Condition

The event-triggering mechanism in S-Q case is based on the true value of sampling of the measurement $y(jh)$ and is evaluated periodically. Inspired by [14], in which the quantization was not considered, the event-triggering condition is given by

$$\begin{aligned}
&\Upsilon^{SQ}(e(jh), y(jh)) \\
&= \gamma W^2(e(jh)) - \pi\rho(\pi)\varepsilon_y \max\{|y(jh)|^2, \Delta_0^2\} \quad (26)
\end{aligned}$$

where

$$\rho(\pi) = \frac{\pi\gamma}{\epsilon(1 - \pi L_{\varepsilon_y})} \quad (27)$$

with

$$\pi \leq \pi^* = \min\left\{1, \frac{\epsilon}{\gamma + \epsilon L_{\varepsilon_y}}\right\} \quad (28)$$

and γ, L_{ε_y} are defined in Assumption 3 and $\epsilon \in (0, 1)$. The sampling period h is chosen such that

$$h \leq \mathcal{T}(\rho(\pi), \gamma, \tilde{L}_W) \quad (29)$$

where

$$\mathcal{T}(\rho(\pi), \gamma, \tilde{L}_W) = \begin{cases} \frac{1}{\tilde{L}_W r}\arctan(\vartheta), & \gamma > \tilde{L}_W \\ \frac{1}{\tilde{L}_W}\frac{1-\rho(\pi)}{1+\rho(\pi)}, & \gamma = \tilde{L}_W \\ \frac{1}{\tilde{L}_W r}\mathrm{arctanh}(\vartheta), & \gamma < \tilde{L}_W \end{cases} \quad (30)$$

and where

$$r := \sqrt{\left|\left(\frac{\gamma}{\tilde{L}_W}\right)^2 - 1\right|},$$

$$\vartheta := \frac{r(1-\rho(\pi))}{\frac{2\rho(\pi)}{1+\rho(\pi)}(\frac{\gamma}{\tilde{L}_W}-1)+1+\rho(\pi)},$$

and $\tilde{L}_W = L_W + \nu$ with $\nu > 0$ any positive small constant. When $\nu = 0$, $\mathcal{T}(\rho(\pi), \gamma, L_W) := T_{\rm MASP}(\pi)$ corresponds to the *maximum allowable sampling period* (MASP). Since the function $\mathcal{T}(\rho(\pi), \gamma, \tilde{L}_W)$ is decreasing in $\tilde{L}_W$, we have $h \leq \mathcal{T}(\rho(\pi), \gamma, \tilde{L}_W) < T_{MASP}(\pi)$. We refer the readers to [29] for more details about MASP. In fact, $\mathcal{T}(\rho(\pi), \gamma, \tilde{L}_W)$ denotes the time it takes for the function $\dot{\phi}(\tau) = -2\tilde{L}_W\phi(\tau) - \gamma(\phi^2(\tau)+1)$ to decrease from $\phi(0) = \frac{1}{\rho(\pi)}$ to $\rho(\pi)$. In this paper, we select $\phi(0) = \frac{1}{\rho(\pi)}$. It is easy to know that $\phi(h) > \rho(\pi)$ if h is chosen to satisfy (29).

C. Stability Analysis

In this section, we are looking for a bounded set of which the system is ISS with respect to disturbance. Before we start the stability analysis, we first define the following set.

Definition 3: We define the following set $\mathcal{A}$:=$\{\xi \in \mathbb{X} : R(\xi) \leq c\}$, where

$$R(\xi) := V(x) + \max\{\gamma\phi(\tau)W^2(e), \pi\varepsilon_y|y|^2, \pi\varepsilon_y|\Delta_0|^2\} \quad (31)$$

$$\dot{\phi}(\tau) = -2\tilde{L}_W\phi(\tau) - \gamma(\phi^2(\tau)+1) \quad (32)$$

$$V(x) = x^T P x \quad (33)$$

and $c := \varepsilon_c\Delta_0^2$ with Δ_0 as mentioned in (26), P positive definite, and $\varepsilon_c > \pi\varepsilon_y + \frac{\gamma\lambda_{\max}(P)}{\rho(\pi)\alpha_V}$.

The following lemmas help proceed with the stability analysis.

Lemma 1: Consider the quantizer strategy in (22)–(24). For each solution pair (ξ, w) with $w \in \mathcal{L}_\infty$, it holds that, when $p(t,j) = 1$:

$$|y| \leq M\mu(t,j), \quad (34)$$

$$\max\{|y|, \Delta_0\} \geq \ell_{\rm in}\mu(t,j). \quad (35)$$

The proof of Lemma 1 could be found in Corollary 1 and Claim 2 in [20].

Lemma 2: Consider the dynamic quantizer with strategy in (22)-(24), and the condition of quantization regions in (25). For each solution pair (ξ, w) with $w \in \mathcal{L}_\infty$, it holds that, when $p(t,j) = 1$:

$$W^2(e_q(t,j)) \leq \rho^2(\pi)W^2(e(t,j)). \quad (36)$$

Proof: In view of (25), we have

$$M - \kappa\Delta \geq \frac{\overline{\alpha}_W\sqrt{\gamma}}{\Omega_{\rm in}\sqrt{\pi\rho^3(\pi)\varepsilon_y}}\Delta.$$

Recalling the definition of $\ell_{\rm in}$ in (23), we obtain $\ell_{\rm in}^2 \geq \frac{\overline{\alpha}_W^2\gamma}{\pi\rho^3(\pi)\varepsilon_y}\Delta^2$. Multiply its both sides by $\mu(t,j)$, we have $\ell_{\rm in}^2\mu^2(t,j) \geq \frac{\overline{\alpha}_W^2\gamma}{\pi\rho^3(\pi)\varepsilon_y}\Delta^2\mu^2(t,j) \geq \frac{\overline{\alpha}_W^2\gamma}{\pi\rho^3(\pi)\varepsilon_y}|e_q|^2$. Hence, in view of Lemma 1 and the event-triggering condition (26), we obtain that for all $\xi \in \mathcal{D}$ when $p(t,j) = 1$:

$$\begin{aligned} W^2(e_q(t,j)) &\leq \overline{\alpha}_W^2|e_q|^2 \\ &\leq \frac{\pi\rho^3(\pi)\varepsilon_y}{\gamma}\ell_{\rm in}^2\mu^2(t,j) \\ &\leq \frac{\pi\rho^3(\pi)\varepsilon_y}{\gamma}\max\{|y|^2, \Delta_0^2\} \\ &\leq \rho^2(\pi)W^2(e(t,j)). \end{aligned} \quad (37)$$

This ends the proof of Lemma 2. ■

Remark 2: Due to the quantization effect, the total network-induced error is not reset to 0 after each transmission. Lemma 2 provides an explicit expression of the upper bound on the total network-induced error right after transmission. Since $\rho(\pi) < 1$, Lemma 2 also shows that the transmitted measurement is more accurate than the information available at the controller side in the sense that $W^2(e(t_k^+)) = W^2(e_q(t_k)) \leq W^2(e(t_k))$. By decreasing the value of $\rho(\pi)$, the effectiveness of each transmission can be improved in the sense that the upper bound is decreasing, with the cost of more quantization regions in the design of dynamic quantizer in (25).

Now we are ready to present the main result.

Theorem 1: Consider the system (12) with the flow and jump sets as in (11). Let $\pi \in (0, \pi^*)$, where π^* is defined in (28). Suppose that Assumptions 1-3 hold, the periodic event-triggered strategy is designed as in (26)–(30), and the dynamic quantizer is designed as in (22)–(24), (25), then the set $\mathcal{A}$ mentioned in *Definition 3* is ISS with respect to the disturbance w.

Proof: Note that we sometimes omit the term (t,j) for simplicity of writing. To prove the ISS property of the set $\mathcal{A}$, we aim to find an ISS Lyapunov function U for the hybrid system (12). We define the function

$$U(\xi) := \max\{0, R(\xi) - c\} \quad (38)$$

with $R(\xi)$ defined in (31). We first show that U constitutes an appropriate candidate ISS Lyapunov function. Notice that $U(\xi) = 0$ for $\xi \in \mathcal{A}$. Since $y = g_p(x_p)$ where g_p is continuous and $g_p(0) = 0$, there exist $\alpha_y \in \mathcal{K}_\infty$ such that $|y|^2 \leq \alpha_y(x)$. In view of the Assumptions 2 and 3 and the definition of $\phi(\tau)$, we deduce that there exist $\overline{\alpha}_U$, $\underline{\alpha}_U \in \mathcal{K}_\infty$ such that:

$$\underline{\alpha}_U(|\xi|_{\mathcal{A}}) \leq U(\xi) \leq \overline{\alpha}_U(|\xi|_{\mathcal{A}}). \quad (39)$$

Next we exploit the dynamic properties of U during flows and jumps.

Dynamics of U during flows: According to the forms of the function $R(\xi)$, we distinguish several cases:
Case 1: $\gamma\phi(\tau)W^2(e) \geq \max\{\pi\varepsilon_y|y|^2, \pi\varepsilon_y\Delta_0^2\}$.

We have that $R(\xi) = V(x) + \gamma\phi(\tau)W^2(e)$. By virtue of Assumptions 2 and 3, we obtain

$$\begin{aligned}
&R^\circ(\xi; F(\xi,w))\\
&\le -\alpha_V|x|^2 + \sigma_V|w|^2 + \gamma^2W^2(e) - H^2(x,e,w) - \varepsilon_y|y|^2\\
&\quad - J(x,e,w) + 2\gamma\phi(\tau)W(e)(L_W W(e) + H(x,e,w))\\
&\quad + \gamma W^2(e)\big(-2L_W\phi(\tau) - \nu\phi(\tau) - \gamma(\phi^2(\tau)+1)\big)\\
&\le -\alpha_V|x|^2 + \sigma_V|w|^2 - \nu\gamma\phi(\tau)W^2(e) - \varepsilon_y|y|^2\\
&\quad - J(x,e,w) - \big(H(x,e,w) - \gamma\phi(\tau)W^2(e)\big)\\
&\le -\alpha_V|x|^2 - \nu\gamma\phi(\tau)W^2(e) + \sigma_V|w|^2\\
&\le -\rho_1(R(\xi)) + \sigma_V|w|^2 \qquad (40)
\end{aligned}$$

where $\rho_1 = \min\Big\{\frac{\alpha_V}{\lambda_{\max}(P)}, \nu\Big\}$.

Case 2: $\gamma\phi(\tau)W^2(e) < \max\{\pi\varepsilon_y|y|^2, \pi\varepsilon_y\Delta_0^2\}$.

Case 2.1: $|y|^2 > \Delta_0^2$.

We have $\gamma\phi(\tau)W^2(e) < \pi\varepsilon_y|y|^2$, and $R(\xi) = V(x) + \pi\varepsilon_y|y|^2$ in this case. Since $\pi < \pi^*$, we have $1 - \pi L_{\varepsilon_y} > \frac{\gamma}{\gamma+\epsilon L_{\varepsilon_y}} > 0$, and

$$\begin{aligned}
&R^\circ(\xi; F(\xi,w))\\
&\le -\alpha_V|x|^2 + \sigma_V|w|^2 + \gamma^2W^2(e) - \varepsilon_y|y|^2 - J(x,e,w)\\
&\quad + \pi\big(L_{\varepsilon_y}\varepsilon_y|y|^2 + H^2(x,e,w) + J(x,e,w)\big) - H^2(x,e,w)\\
&= -\alpha_V|x|^2 + \gamma^2W^2(e) - (1-\pi L_{\varepsilon_y})\varepsilon_y|y|^2 + \sigma_V|w|^2\\
&\quad - (1-\pi)\big(H^2(x,e,w) + J(x,e,w)\big)\\
&\le -\alpha_V|x|^2 + \gamma^2W^2(e) - (1-\pi L_{\varepsilon_y})\varepsilon_y|y|^2\sigma_V|w|^2.
\end{aligned}$$

Since $\phi(\tau) > \rho(\pi)$, we obtain $\gamma^2W^2(e) = \frac{\gamma\phi(\tau)W^2(e)}{\phi(\tau)} \le \frac{\gamma\pi\varepsilon_y|y|^2}{\phi(\tau)} \le \frac{\gamma\pi\varepsilon_y|y|^2}{\rho(\pi)} = \epsilon(1-\pi L_{\varepsilon_y})\varepsilon_y|y|^2$. Then it follows that for $\epsilon \in (0,1)$

$$\begin{aligned}
&R^\circ(\xi; F(\xi,w))\\
&\le -\alpha_V|x|^2 - (1-\epsilon)(1-\pi L_{\varepsilon_y})\varepsilon_y|y|^2 + \sigma_V|w|^2\\
&\le -\rho_2 R(\xi) + +\sigma_V|w|^2 \qquad (41)
\end{aligned}$$

where $\rho_2 = \min\Big\{\frac{\alpha_V}{\lambda_{\max}(P)}, \frac{(1-\epsilon)(1-\pi L_{\varepsilon_y})}{\pi}\Big\}$.

Case 2.2: $\Delta_0^2 \ge |y|^2$.

Then it gives that $\gamma\phi(\tau)W^2(e) \le \pi\varepsilon_y\Delta_0^2$, and $R(\xi) = V(x) + \pi\varepsilon_y\Delta_0^2$. Since $\gamma^2W^2(e) = \frac{\gamma\phi(\tau)W^2(e)\gamma}{\phi} \le \frac{\gamma\Delta_0^2}{\phi(\tau)} \le \frac{\gamma\Delta_0^2}{\rho(\pi)}$, in view of Assumption 3, we obtain

$$\begin{aligned}
&R^\circ(\xi; F(\xi,w))\\
&\le -\alpha_V|x|^2 + \sigma_V|w|^2 + \gamma^2W^2(e) - \varepsilon_y|y|^2\\
&\quad - J(x,e,w) - H^2(x,e,w)\\
&\le -\alpha_V|x|^2 + \sigma_V|w|^2 + \gamma^2W^2(e)\\
&\le -\frac{\alpha_V}{\lambda_{\max(\mathrm{P})}}V(x) + \frac{\gamma\Delta_0^2}{\rho(\pi)} + \sigma_V|w|^2.
\end{aligned}$$

For simplicity of expression, let $b_1 = \pi\varepsilon_y$, $b_2 = \frac{\gamma}{\rho(\pi)}$, $b_3 = \frac{\alpha_V}{\lambda_{\max(\mathrm{P})}}$, $\rho_3 = \frac{(\varepsilon_c - b_1)b_3 - b_2}{\varepsilon_c}$. It could be verified that $\varepsilon_c - b_1 = \frac{b_2+\rho_3 b_1}{c_1-\rho_3}$. Since $R(\xi) > c$, we have $V(x) > (\varepsilon_c - b_1)\Delta_0^2 = \frac{b_2+\rho_3 b_1}{b_3-\rho_3}\Delta_0^2$. By simple mathematical transformation, we obtain $-b_3V(x) + b_2\Delta_0^2 < -\rho_3(V(x) + b_1\Delta_0^2)$. Finally we obtain

$$\begin{aligned}
R^\circ(\xi; F(\xi,w)) &\le -b_3V(x) + b_2\Delta_0^2 + +\sigma_V|w|^2\\
&\le -\rho_3 R(\xi) + \sigma_V|w|^2.
\end{aligned}$$

In view of the above cases, we obtain that for all $\xi(t,j) \in \mathcal{C}\backslash\mathcal{A}$

$$R^\circ(\xi; F(\xi,w)) \le -\rho_0 R(\xi) + \sigma_V|w|^2 \qquad (42)$$

where $\rho_0 = \min\{\rho_1, \rho_2, \rho_3\}$. Recall that $U(\xi) = 0$ when $\xi \in \mathcal{A}$, we can conclude that for all $\xi(t,j) \in \mathcal{C}$

$$U^\circ(\xi; F(\xi,w)) \le -\rho_0 U(\xi) + \sigma_V|w|^2. \qquad (43)$$

Dynamics of U during jump sets: We distinguish three cases according to the jump maps in (14).

Case 1: $\xi \in G_0^{SQ}(\xi)$.

By virtue of the event-triggering condition, we have $\gamma W^2(e) < \pi\rho(\pi)\varepsilon_y\max\{|y|^2, \Delta_0^2\}$. Note that $\rho(\pi) \in (0,1)$ ensured by $\pi \le \pi^* \le 1$. Define $\varpi = \max\{|y|^2, \Delta_0^2\}$ for simplicity of writing. Recall that $\phi(0) = \frac{1}{\rho(\pi)}$, we have

$$\begin{aligned}
R(G_0^{SQ}(\xi)) &= V(x) + \max\big\{\gamma\phi(0)W^2(e), \pi\varepsilon_y|y|^2, \pi\varepsilon_y\Delta_0^2\big\}\\
&= V(x) + \max\big\{\gamma\phi(0)W^2(e), \pi\varepsilon_y\varpi\big\}\\
&\le V(x) + \max\{\phi(0)\pi\rho(\pi)\varepsilon_y\varpi, \pi\varepsilon_y\varpi\}\\
&\le V(x) + \pi\varepsilon_y\varpi\\
&\le R(\xi). \qquad (44)
\end{aligned}$$

Case 2: $\xi \in G_\mu^{SQ}(\xi)$.

In this case, the jump only changes the values of μ and p. It is easy to verify that

$$R(G_\mu^{SQ}(\xi)) \le R(\xi). \qquad (45)$$

Case 3: $\xi \in G_y^{SQ}(\xi)$.

By using Lemma 2 and the fact that $\phi(h) > \rho(\pi)$, we have

$$\begin{aligned}
R(G_y^{SQ}(\xi)) &= V(x) + \max\big\{\gamma\phi(0)W^2(e_q), \pi\varepsilon_y|y|^2, \pi\varepsilon_y\Delta_0^2\big\}\\
&\le V(x) + \max\big\{\gamma\rho^2(\pi)\phi(0)W^2(e), \pi\varepsilon_y\varpi\big\}\\
&\le V(x) + \max\big\{\gamma\phi(h)W^2(e), \pi\varepsilon_y\varpi\big\}\\
&= R(\xi). \qquad (46)
\end{aligned}$$

By combining three cases above, it holds that $R(G^{SQ}(\xi)) \le R(\xi)$ when $\xi(t,j) \in \mathcal{D}$. When $\xi(t,j) \in \mathcal{D}\backslash\mathcal{A}$, we have $U(G^{SQ}(\xi)) = \max\{0, R(G^{SQ}(\xi)) - c\} \le \max\{0, R(\xi) - c\} = U(\xi)$. When $\xi(t,j) \in \mathcal{D} \wedge \xi(t,j) \in \mathcal{A}$, we also have $U(G^{SQ}(\xi)) \le U(\xi)$ since $G^{SQ}(\xi) \in \mathcal{A}$. We thus conclude that for all $\xi(t,j) \in \mathcal{D}$

$$U(G^{SQ}(\xi)) \le U(\xi). \qquad (47)$$

By using standard Lyapunov arguments as in [14], we can draw the conclusion of Theorem 1, which completes the proof. ■

It is worth mentioning that, in our design, the setting of Δ_0 is introduced to deal with the quantized control problem. The selection of Δ_0 is closely related to the practical issues. For one thing, the minimum zoom variable $\mu_{\min} = \frac{\Delta_0\Omega_{\text{in}}}{\ell_{\text{in}}}$ in the dynamic quantizer is based on Δ_0, which is limited by the constrained communication resource, see Remark 3 in [20] for more details. For another, Δ_0 directly determines the size of bounded set $\mathcal{A}$. Moreover, we can show that the amount of data sent over the network is bounded at each transmission through simple calculations, which is omitted here.

Remark 3: The choice of the parameter π plays an essential role in the design of the whole system, which directly affects

the design of the event-triggering mechanism, dynamic quantizer and the time constant h. In the dynamic quantizer side, if we increase π, $\rho(\pi)$ is also increasing, and less quantization regions will be needed in view of (25). From the event-triggering perspective, large values of π and $\rho(\pi)$ make it less possible to transmit at one sampling instant. However, since the function $\mathcal{T}(\rho(\pi),\gamma,\tilde{L}_W)$ is decreasing in $\rho(\pi)$, the increasing of $\rho(\pi)$ comes with the decreasing of the sampling period. Notice that large values of π and $\rho(\pi)$, which leads to less possibility of transmission at one sampling instant, will not necessarily lead to large average inter-transmission times since the sampling is implemented more frequently. In fact, more frequent sampling usually causes large average inter-transmission time as we will show in the simulation section. As we can see, the trade-off among the transmission, quantization and sampling period can be characterized in terms of the design parameter π.

IV. Main Results: Quantization Before Sampling (Q-S) Case

In this section, we concentrate on the Q-S case. We aim to exploit the methodology to jointly design the quantizer and event-triggering mechanism to ensure the stability property.

Recall that in the Q-S case the quantization process is done before the event-triggering detection. Therefore, the data that is available in the event-trigger processing unit, i.e., quantized measurement, is rougher than that in S-Q case (non-quantized measurement), which constitutes one of the challenges in the stability analysis. In fact, we usually need a higher transmission frequency and more quantization regions to compensate the drawbacks induced by the rougher data, as we will discuss in the following part.

A. Design of the Dynamic Quantizer

For the design of dynamic quantizer, we use the same quantization strategy as in S-Q case (22)-(24). To guarantee the ISS property, the number of quantization regions is required as follows:

$$\frac{M}{\Delta} \geq \kappa + \frac{1}{\Omega_{\text{in}}}\max\left\{\sqrt{\frac{\mathrm{c}_2}{\mathrm{c}_1}},\sqrt{\frac{\mathrm{c}_3}{\mathrm{c}_4}}\right\} \tag{48}$$

where

$$\begin{aligned} c_1 &= \frac{\pi\varepsilon_y\rho(\pi)}{\gamma\overline{\alpha}_W^2}\left(1-\frac{(1+\kappa_q)\overline{\alpha}_W^2(1+\kappa_e)}{\delta\underline{\alpha}_W^2}\right)\\ c_2 &= \left(\left(1+\frac{1}{\kappa_e}\right)+\frac{\left(1+\frac{1}{\kappa_q}\right)(1+\kappa_e)}{\delta\gamma\underline{\alpha}_W^2}\right)\\ c_3 &= \left(\frac{\overline{\alpha}_W^2}{\rho^2(\pi)\underline{\alpha}_W^2}-\left(1-\frac{1}{\kappa_e}\right)\right)\\ c_4 &= \frac{(1-\kappa_e)(1-\kappa_q)\pi\rho(\pi)\varepsilon_y}{\delta\gamma\overline{\alpha}_W^2} \end{aligned} \tag{49}$$

and $\kappa_e\in(0,1)$, $\kappa_q\in(0,1)$ are two parameters to be designed, π, $\rho(\pi)$, δ are parameters in the event-triggering mechanism and will be specified in the subsequent part.

Remark 4: There is an observation that the required number of quantization regions of Q-S case in (48) is always greater than that of S-Q case in (25). In view of the definition of c_3, c_4, since $\kappa_q\in(0,1)$, $\kappa_e\in(0,1)$, we obtain that $c_3 > \frac{\overline{\alpha}_W^2}{\rho^2(\pi)\underline{\alpha}_W^2}$, $c_4 < \frac{\pi\rho(\pi)\varepsilon_y}{\delta\gamma\underline{\alpha}_W^2}$. Hence, $\frac{c_3}{c_4} > \frac{\overline{\alpha}_W^2\gamma}{\pi\rho^3(\pi)\varepsilon_y}\frac{\delta\overline{\alpha}_W^2}{\underline{\alpha}_W^2} > \frac{\overline{\alpha}_W^2\gamma}{\pi\rho^3(\pi)\varepsilon_y}$. Therefore, we have $\frac{M}{\Delta}\geq\kappa+\frac{1}{\Omega_{\text{in}}}\sqrt{\frac{c_3}{c_4}}\geq\kappa+\frac{\overline{\alpha}_W\sqrt{\gamma}}{\Omega_{in}\sqrt{\pi\rho^3(\pi)\varepsilon_y}}$, which verifies our opinion.

B. Design of the Event-Triggering Condition

The event-triggering condition in Q-S case is designed as

$$\begin{aligned} &\Upsilon^{QS}(e_s(jh),q_\mu(y(jh)))\\ &=\delta\gamma W^2(e_s(jh))-\pi\rho(\pi)\varepsilon_y\max\{|q_\mu(y(jh))|^2,\Delta_0^2\} \end{aligned} \tag{50}$$

where

$$\rho(\pi)=\frac{\pi\gamma}{\epsilon(1-\pi L_{\varepsilon_y})} \tag{51}$$

with

$$\pi\leq\pi^*=\min\{1,\frac{\epsilon}{\gamma+\epsilon L_{\varepsilon_y}}\} \tag{52}$$

$$\delta>\frac{(1+\kappa_q)(1+\kappa_e)\overline{\alpha}_W^2}{\underline{\alpha}_W^2} \tag{53}$$

and γ, L_{ε_y} are defined in Assumption 3 and $\epsilon\in(0,1)$. The method to design the sampling period h is the same as that in S-Q case, see (29) in Section III.B.

Remark 5: Compared with the S-Q event-triggering mechanism in (26), an obvious difference is the introduction of the parameter δ. $\delta>1$ means that the event-triggering mechanism in (50) is more likely to be activated. It makes sense as we need more frequent communication between the controller and the plant to make the controller keep pace with the plant when the quantization effect, which can be seen as some uncertainty, disturbs the accuracy of output measurement.

C. Stability Analysis

Theorem 2: Consider the system (17) with the flow and jump sets as in (11). Let $\pi\in(0,\pi^*)$, where π^* is defined in (52). Suppose that Assumptions 1–3 hold, the periodic event-triggered strategy is designed as in (50)–(53),(29), the dynamic quantizer is designed as in (48)–(49), (22)–(24), then the set $\mathcal{A}$ in *Definition 3* is ISS with respect to the disturbance w.

Proof: Our aim is to prove the function U in (38) satisfies (39), (43), and (47). The proof of (39) and (43) is the same as in the proof of Theorem 1 and thus omitted. Note that we denote $q_\mu(y)$ as q for simplicity of writing. We focus on the jump sets when $\xi\in\mathcal{D}$, and distinguish three cases according to the event-triggering condition.

Case 1: $\xi\in G_0^{QS}(\xi)$.

Then we have $\delta\gamma W^2(e_s) < \pi\rho(\pi)\varepsilon_y\max\{|q_\mu(y)|^2,\Delta_0^2\}$, and $p(t,j)=1$. Next We present the following facts that is easy to be verified and will be used later.

Fact 1: $|e|\leq|e_q|+|e_s|$, from which we have $|e|^2\leq(1+\kappa_e)|e_s|^2+\left(1+\frac{1}{\kappa_e}\right)|e_q|^2$ with $\kappa_e\in(0,1)$.

Fact 2: $|q|\leq|y|+\Delta\mu(t,j)$, from which we have $|q|^2\leq(1+\kappa_q)|y|^2+\left(1+\frac{1}{\kappa_q}\right)\Delta^2\mu^2$ with $\kappa_q\in(0,1)$.

From (48), we obtain $\frac{M}{\Delta}\geq\kappa+\frac{1}{\Omega_{\text{in}}}\sqrt{\frac{c_2}{c_1}}$, i.e., $\frac{\ell_{\text{in}}^2}{\Delta^2}\geq\frac{c_2}{c_1}$. Since the quantization strategy (22)-(24) is utilized in the

Q-S case, Lemma 1 can also be applied. Then we have $c_2\Delta^2\mu^2(t,j) \leq c_1\ell_{\text{in}}^2\mu^2(t,j) \leq c_1\max\{|y|^2,\Delta_0^2\}$. Define $\varpi = \max\{|y|^2,\Delta_0^2\}$. Recalling the definition of c_1, c_2 in (49), we can obtain through simple transformation that

$$\begin{aligned}&\frac{\pi\rho(\pi)\varepsilon_y\varpi(1+\kappa_q)+\left(1+\frac{1}{\kappa_q}\right)\Delta^2\mu^2(t,j)}{\delta\gamma\underline{\alpha}_W^2}\\ \leq&\frac{\frac{\pi\rho(\pi)\varepsilon_y}{\gamma\overline{\alpha}_W^2}\varpi-\left(1+\frac{1}{\kappa_e}\right)\Delta^2\mu^2(t,j)}{1+\kappa_e}.\end{aligned}\tag{54}$$

By virtue of Fact 2, and the event-triggering condition (50), it follows that

$$\begin{aligned}&\pi\rho(\pi)\varepsilon_y\varpi(1+\kappa_q)+\left(1+\frac{1}{\kappa_q}\right)\Delta^2\mu^2(t,j)\\ &=\pi\rho(\pi)\varepsilon_y(1+\kappa_q)\max\left\{|y|^2,\Delta_0^2\right\}+\left(1+\frac{1}{\kappa_q}\right)\Delta^2\mu^2(t,j)\\ &\geq\pi\rho(\pi)\varepsilon_y\max\left\{(1+\kappa_q)|y|^2,\Delta_0^2\right\}+\left(1+\frac{1}{\kappa_q}\right)\Delta^2\mu^2(t,j)\\ &\geq\pi\rho(\pi)\varepsilon_y\max\left\{(1+\kappa_q)|y|^2+\left(1+\frac{1}{\kappa_q}\right)\Delta^2\mu^2(t,j),\Delta_0^2\right\}\\ &\geq\pi\rho(\pi)\varepsilon_y\max\left\{|q|^2,\Delta_0^2\right\}\\ &\geq\delta\gamma W^2(e_s)\\ &\geq\delta\gamma\underline{\alpha}_W^2|e_s|^2.\end{aligned}\tag{55}$$

Combining (54)–(55) with Fact 1, we obtain

$$\begin{aligned}W^2(e)&\leq\overline{\alpha}_W^2|e|^2\\ &\leq\overline{\alpha}^2\left((1+\kappa_e)|e_s|^2+\left(1+\frac{1}{\kappa_e}\right)|e_q|^2\right)\\ &\leq\frac{\pi\rho(\pi)\varepsilon_y}{\gamma}\varpi.\end{aligned}\tag{56}$$

Finally it holds that

$$\begin{aligned}R(G_0^{QS}(\xi))&=V(x)+\max\left\{\gamma\phi(0)W^2(e),\pi\varepsilon_y\varpi\right\}\\ &\leq V(x)+\pi\varepsilon_y\varpi\\ &\leq R(\xi).\end{aligned}\tag{57}$$

Case 2: $\xi\in G_\mu^{QS}(\xi)$.

Observe that the values of the variables x, e, τ do not change. The following can be easily verified

$$R(G_\mu^{QS}(\xi))\leq R(\xi).\tag{58}$$

Case 3: $\xi\in G_y^{QS}(\xi)$.

Then we have $\delta\gamma W^2(e_s)>\pi\rho(\pi)\varepsilon_y\max\{|q_\mu(\mathrm{y})|^2,\Delta_0^2\}$, and $p(t,j)=1$. The following two facts are easily verified.

Fact 3: $|e|\geq|e_s|-|e_q|$, from which we have $|e|^2\geq(1-\kappa_e)|e_s|^2+\left(1-\frac{1}{\kappa_e}\right)|e_q|^2$ with $\kappa_e\in(0,1)$.

Fact 4: $|q|\geq|y|-\Delta\mu$, from which we have $|q|^2\geq(1-\kappa_q)|y|^2+\left(1-\frac{1}{\kappa_q}\right)\Delta^2\mu^2(t,j)$ with $\kappa_q\in(0,1)$.

From (48), we can obtain $\frac{M}{\Delta}\geq\kappa+\frac{1}{\Omega_{\text{in}}}\sqrt{\frac{c_3}{c_4}}$, i.e., $\frac{\ell_{\text{in}}^2}{\Delta^2}\geq\frac{c_3}{c_4}$. Recalling the definition of c_3, c_4 in (49), we can obtain through a simple transformation that

$$\begin{aligned}&\frac{\overline{\alpha}_W^2}{\rho^2(\pi)\underline{\alpha}_W^2}\Delta^2\mu^2(t,j)-\left(1-\frac{1}{\kappa_e}\right)\Delta^2\mu^2(t,j)\\ &\leq\frac{(1-\kappa_e)(1-\kappa_q)\pi\rho(\pi)\varepsilon_y}{\delta\gamma\overline{\alpha}_W^2}\varpi.\end{aligned}\tag{59}$$

By virtue of the event-triggering condition (50) and Fact 4, we obtain that

$$\begin{aligned}&\pi\rho(\pi)\varepsilon_y(1-\kappa_q)\max\left\{|y|^2,\Delta_0^2\right\}\\ &\leq\pi\rho(\pi)\varepsilon_y\max\left\{(1-\kappa_q)|y|^2,\Delta_0^2\right\}\\ &\leq\pi\rho(\pi)\varepsilon_y\max\left\{(1-\kappa_q)|y|^2+\left(1-\frac{1}{\kappa_q}\right)\Delta^2\mu^2,\Delta_0^2\right\}\\ &\leq\pi\rho(\pi)\varepsilon_y\max\left\{|q|^2,\Delta_0^2\right\}\\ &\leq\delta\gamma W^2(e_s)\\ &\leq\delta\gamma\overline{\alpha}_W^2|e_s|^2.\end{aligned}\tag{60}$$

In view of (59)–(60) and Fact 3, it gives that

$$\begin{aligned}&\frac{\overline{\alpha}_W^2}{\rho^2(\pi)\underline{\alpha}_W^2}|e_q|^2\\ &\leq\left(1-\frac{1}{\kappa_e}\right)|e_q|^2+(1-\kappa_e)|e_s|^2\\ &\leq|e|^2.\end{aligned}\tag{61}$$

Then, we have

$$\begin{aligned}R(G_y^{QS}(\xi))&=V(x)+\max\left\{\gamma\phi(0)W^2(e_q),\pi\varepsilon_y\varpi\right\}\\ &\leq V(x)+\max\left\{\gamma\frac{\overline{\alpha}_W^2}{\rho(\pi)}|e_q|^2,\pi\varepsilon_y\varpi\right\}\\ &\leq V(x)+\max\left\{\gamma\rho(\pi)\underline{\alpha}_W^2|e|^2,\pi\varepsilon_y\varpi\right\}\\ &\leq V(x)+\max\left\{\gamma\phi(\tau)W^2(e),\pi\varepsilon_y\varpi\right\}\\ &=R(\xi).\end{aligned}\tag{62}$$

As a result, it holds that for all $\xi\in\mathcal{D}$

$$U(G^{QS}(\xi))\leq U(\xi)\tag{63}$$

which completes the proof by using standard Lyapunov arguments as in [14]. ■

Remark 6: For a fixed π, if we choose the same value of sampling period h, we could decrease the parameter δ to increase the inter-transmission times. Recalling the definitions of c_1, c_2, c_3, c_4, in (49), when δ approaches infinity, we have $\frac{c_2}{c_1}\geq\frac{\overline{\alpha}_W^2\gamma(1+\frac{1}{\kappa_e})}{\pi\rho(\pi)\varepsilon_y}$. We sketch the functions $\frac{c_2}{c_1}$ and $\frac{c_3}{c_4}$ depending on δ. As shown in Fig 3, the decreasing of δ comes with the decreasing of $\frac{c_3}{c_4}$ and the increasing of $\frac{c_2}{c_1}$, which may lead to increased number of quantization regions in view of the quantizer condition (48). Therefore, there also exist a trade-off between the transmission and quantization in terms of the parameter δ.

We observe that, compared with the S-Q case, the Q-S case needs more frequent communication and more quantization regions to stabilize the closed-loop system, see Remark 4 and Remark 5 for more discussions. We give an intuitive explanation for the phenomenon: In the quantization before sampling case, the sensor measurement is first influenced by quantization effect which can be seen as some kind of

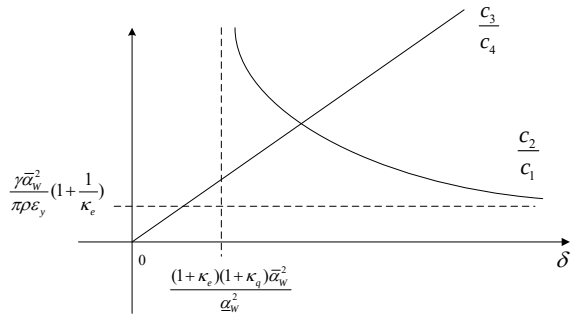

Fig. 3. An illustration of the changes of $\frac{c_3}{c_4}$ and $\frac{c_2}{c_1}$ in terms of the parameter δ.

disturbance with an upper bound determined by the dynamic quantizer, and then utilized for checking the event-triggering condition to decide when to transmit information. From this perspective, the Q-S case can be seen as a worst case of the S-Q case and naturally pays more costs for the stability guarantee.

V. Illustrative Example

In this section, we provide a numerical example to verify the theoretical results in Section III and IV. We consider a single-link robot arm example [9], and the system dynamics is given by

$$\begin{aligned} \dot{x}_p &= A_p x_p + B_p u - B_p \psi(y) + E_p w \\ y &= C_p x_p \end{aligned} \tag{64}$$

where $A_p = \begin{bmatrix} 0 & 1 \\ 0 & 0 \end{bmatrix}$, $B_p = \begin{bmatrix} 0 \\ 1 \end{bmatrix}$, $E_p = \begin{bmatrix} 0 \\ 1 \end{bmatrix}$, $C_p = \begin{bmatrix} 1 & 0 \end{bmatrix}$, $\psi(y) = \sin(y)$. The observer-based controller borrower from [9] is given by :

$$\begin{aligned} \dot{x}_c &= A_p x_c + B_p u - B_p \psi(\hat{y}_q) + M(\hat{y}_q - C_p x_c) \\ u &= K x_c + \psi(\hat{y}_q) \end{aligned} \tag{65}$$

We design the matrix K such that the eigenvalues of $A_p + B_p K$ are -2 and -6, and the matrix M such that the eigenvalues of $A_p - MC_p$ are -1 and -5. Hence, we obtain $K = \begin{bmatrix} -12 & -8 \end{bmatrix}$, $M = \begin{bmatrix} 6 & 5 \end{bmatrix}^T$. We consider the case that the output measurement y is transmitted to the controller over a digital channel and the controller is co-located with the actuator. Let $x = (x_p, x_c)$, $e = \hat{y}_q - y$, we obatin the hybrid model:

$$\begin{aligned} \dot{x} &= \mathcal{A}_1 x + \mathcal{B}_1 e + \mathcal{E}_1 w + D_1 \varphi(y) \\ \dot{e} &= \mathcal{A}_2 x \end{aligned} \tag{66}$$

where $\mathcal{A}_1 = \begin{bmatrix} A_p & B_p K \\ MC_p & A_p + B_p K - MC_p \end{bmatrix}$, $\mathcal{B}_1 = \begin{bmatrix} 0 \\ M \end{bmatrix}$, $\mathcal{E}_1 = \begin{bmatrix} E_p \\ 0 \end{bmatrix}$, $\mathcal{A}_2 = \begin{bmatrix} -C_p A_P & -C_p B_p K \end{bmatrix}$, $D_1 = \begin{bmatrix} 0 & 1 & 0 & 0 \end{bmatrix}$, $\varphi(y) = \psi(\hat{y}_q) - \psi(y)$.

We now verify Assumptions 2 and 3. We take $W(e) = |e|$, then Assumption 2 holds with $\underline{\alpha}_W = \overline{\alpha}_W = 1$, $L_W = 0$, and $H(x, e, w) = |\mathcal{A}_2 x|$. Take $V(x) = x^T P x$, then item 1 of Assumption 3 satisfies with $\underline{\alpha}_V = \lambda_{\min}(P)$, $\overline{\alpha}_V = \lambda_{\max}(P)$. Since $\langle \nabla \varepsilon_y |y|^2, -g(x, e, w) \rangle \leq 2\varepsilon_y |y| |\mathcal{A}_2 x| \leq \varepsilon_y |y|^2 + \varepsilon_y |\mathcal{A}_2 x|^2$, item 3 of Assumption 3 satisfies with $L_{\varepsilon_y} = 1$, $J(x, e, w) = \varepsilon_y |\mathcal{A}_2 x|^2$. We then verify item 2 of Assumption 3. Note that $\varphi(y) = \psi(e + y) - \psi(y) \leq |e|$, we have $2x^T P D_1 \varphi(y) \leq 2|x||P||D_1||\varphi(y)| \leq 2|x||P||D_1||e| \leq \alpha_V |x|^2 + \frac{|P|^2}{\alpha_V} |e|^2$. By Schur Complement Lemma, it is sufficient to make Item 2 of Assumption 3 hold if the following LMI is satisfied:

$$\begin{bmatrix} \Sigma & P\mathcal{B}_1 & P\mathcal{E}_1 \\ * & -\left(\gamma^2 - \frac{|P|^2}{\alpha_V}\right) I_{n_e} & 0 \\ * & * & -\sigma_V I_{n_w} \end{bmatrix} \leq 0 \tag{67}$$

where $\Sigma = P\mathcal{A}_1 + \mathcal{A}_1^T P + 2\alpha_V I_{n_x} + (1+\varepsilon_y)\mathcal{A}_2^T \mathcal{A}_2 + \varepsilon_y D_y^T D_y$ and $D_y = \begin{bmatrix} 1 & 0 & 0 & 0 \end{bmatrix}$ with $y = D_y x$. Observe that (67) is always feasible with a sufficiently large γ since $\mathcal{A}$ is Hurwitz. One way to solve LMI (67) is to select some parameters P, ε_y, α_V, σ_V, η such that the following holds

$$\begin{bmatrix} \Sigma & P\mathcal{B}_1 & P\mathcal{E}_1 \\ * & -\eta I_{n_e} & 0 \\ * & * & -\sigma_V I_{n_w} \end{bmatrix} \leq 0 \tag{68}$$

where Σ is as in (67). Then (67) holds with $\gamma^2 = \eta + \frac{|P|^2}{\alpha_V}$.

By selecting $\varepsilon_y = 2$, $\alpha_V = 1$, $\epsilon = 0.9$, we solve LMI (67) to obtain $\gamma = 93.5179$, $\pi^* = 0.0095$. We choose $\pi = 0.8\pi^*$, which yields $\rho(\pi) = 0.7985$ and $T_{MASP} = 0.0167$. We set the initial conditions $x(0, 0) = (3, 0.5, -3, 0.5)$ and the sampling period $h = 0.01$ and the random disturbance w satisfying $|w(t)| \leq 0.5$ with $t \in [0, 1]$, $w(t) = 0$ with $t \in (1, 3]$ and $|w(t)| \leq 0.2$ with $t \in (3, 5]$.

For the quantization after sampling case, We take $M = 6$, $\Delta = 0.01$, $\Omega_{\text{in}} = 0.5$, $\Omega_{\text{out}} = 2$, $\kappa = 3$, which verify conditions (24), (25) and lead to $\ell_{\text{in}} = 2.985$, $\ell_{\text{out}} = 5.99$. Fig. 4 illustrates the state trajectory of the plant and the controller and the control input. Fig. 5 shows the measurement and zoom actions of the dynamic quantizer, and we can see that the quantizer variable μ is appropriately selected such that the measurement y always stays within $[\ell_{\text{in}}\mu, \ell_{\text{out}}\mu)$. The inter-transmission interval and the inter-zoom interval are illustrated in Fig. 6.

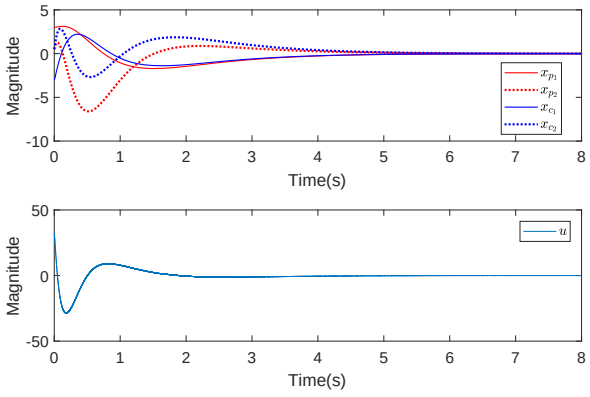

Fig. 4. State trajectories and control input: S-Q case.

For the quantization before sampling case, we select $M = 10$, $\Delta = 0.01$, $\Omega_{\text{in}} = 0.5$, $\Omega_{\text{out}} = 2$, $\kappa = 3$, which verify (24), (48), and $\kappa_q = \kappa_e = 0.4$, $\delta = 2.5$ which verify (53).

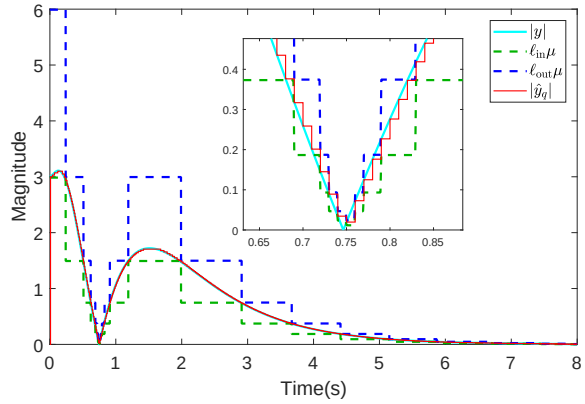

Fig. 5. Zoom actions of the dynamic quantizer: S-Q case

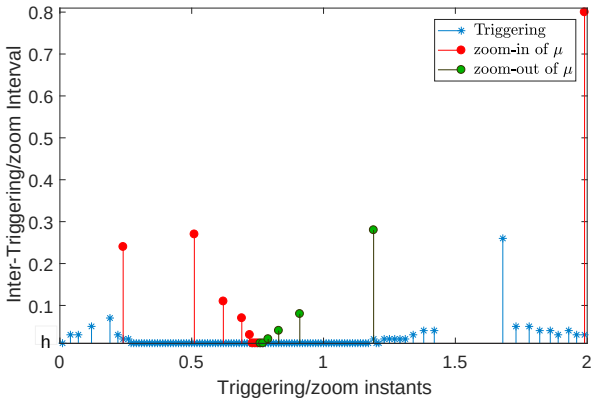

Fig. 6. Triggering/zoom instants for the first two seconds: S-Q case

The state trajectory and control input are illustrated in Fig. 7. The zoom actions of dynamic quantizer and the inter-transmission/zoom intervals are shown in Fig. 8 and Fig. 9 respectively. We observe that Zeno-behavior of transmission and accumulation of zoom actions are both prevented, and the practical implementation is guaranteed. The trade-off for the

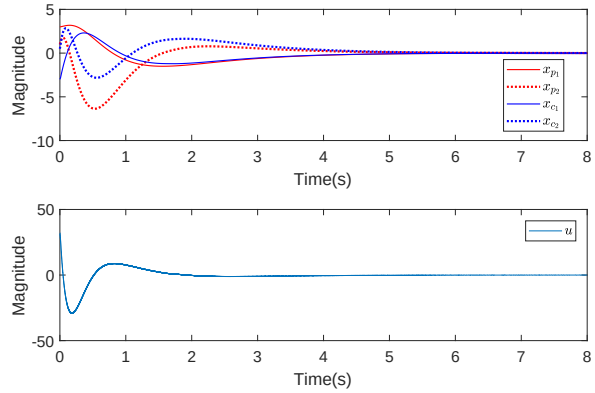

Fig. 7. State trajectories and control input: Q-S case.

S-Q case among the quantization regions, sampling period, and average inter-transmission times is presented in Fig. 10, which is generated by varying the value of π. The Q-S case obtains

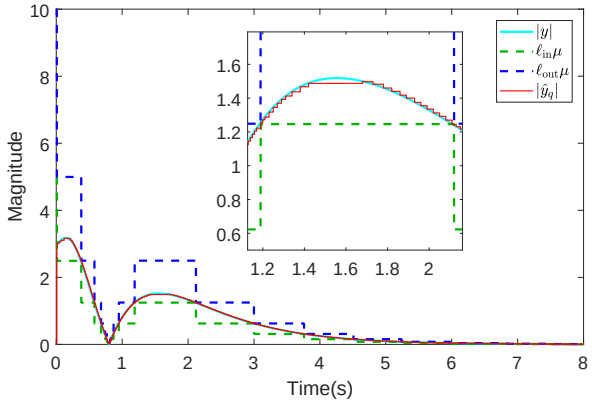

Fig. 8. Zoom actions of the dynamic quantizer: Q-S case

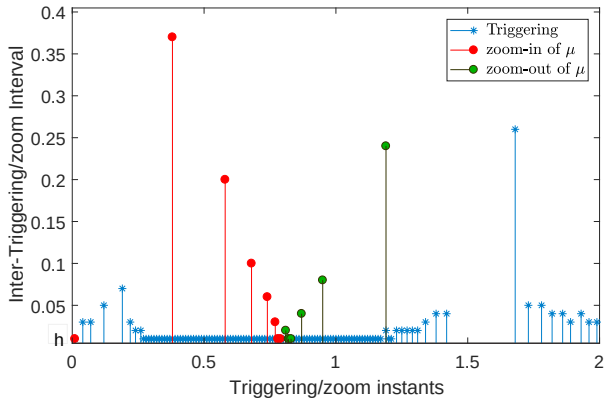

Fig. 9. Triggering/zoom instants for the first two seconds: Q-S case

the similar result and thus omitted. Notice that when the sampling period h is decreasing ($\frac{M}{\Delta}$ is decreasing), the average inter-transmission times increases. When the sampling period h decreases to some extent, the average inter-transmission times rebounds to decrease.

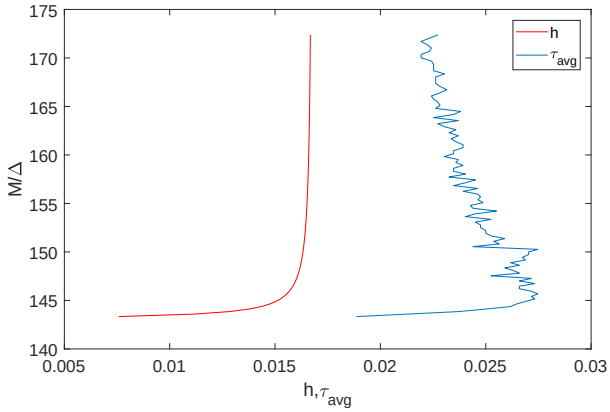

Fig. 10. Trade-off curves among sampling period, quantization regions and average inter-transmission intervals

VI. Conclusion

In order to save communication expenditure in NCS, we exploit both temporal and spatial aspects in this paper, i.e., both the quantization effect and the event-triggering mechanism are considered. We have investigated periodic event-triggered control with quantization effect and external disturbance. Both the quantization after sampling and quantization before sampling cases are studied. The joint design of dynamic quantizer and the event-triggering mechanism is proposed, with Zeno-behavior of transmission and accumulation of zoom instants prevented for both cases. We exploit the hybrid system approach to guarantee the ISS property of a size-adjustable set around the origin, and the trade-off among the transmission, quantization regions and sampling period is characterized in terms of the design parameters.

References

[1] W.P.M.H. Heemels, A.R. Teel, Nathan van de Wouw and D. Nesic, "Networked Control Systems With Communication Constraints: Tradeoffs Between Transmission Intervals, Delays and Performance," *IEEE Transactions on Automatic Control*, vol. 55, no. 8, pp. 1781-1796, Aug. 2010.

[2] M.C.F. Donkers, W.P.M.H. Heemels, Nathan van de Wouw and L. Hetel, "Stability Analysis of Networked Control Systems Using a Switched Linear Systems Approach," *IEEE Transactions on Automatic Control*, vol. 56, no. 9, pp. 2101-2115, Sept. 2011.

[3] P. Tabuada, "Event-Triggered Real-Time Scheduling of Stabilizing Control Tasks," *IEEE Transactions on Automatic Control*, vol. 52, no. 9, pp. 1680-1685, 2007.

[4] X. Wang and M. D. Lemmon, "Event-Triggering in Distributed Networked Control Systems," *IEEE Transactions on Automatic Control*, vol. 56, no. 3, pp. 586-601, 2011.

[5] M.C.F. Donkers and W. P. M. H. Heemels, "Output-based event-triggered control with guaranteed $\mathcal{L}_\infty$ gain and improved and decentralized event triggering," *IEEE Transactions Automatic Control*, vol. 57, no. 6, pp. 1362-1376, Jun. 2012.
Elia2001,Liberzon2007

[6] N. Elia and S. K. Mitter, "Stabilization of linear systems with limited information," *IEEE Transactions on Automatic Control*, vol. 46, pp.1384-1400, 2001.

[7] D. Liberzon and D. Nesic, "Input-to-state stabilization of linear systems with quantized state measurements," *IEEE Transactions on Automatic Control*, vol. 52, no. 5, pp. 767-781, May 2007.

[8] V.S.Dolk, D. Borgers, and W. Heemels, "Output-based and decentralized dynamic ETC with guaranteed $\mathcal{L}_P$-gain performance and zeno-freeness," *IEEE Transactions Automatic Control*, vol. 62, pp. 34-49, 2017.

[9] M. Abdelrahim, R. Postoyan, J. Daafouz, and D. Nesic, "Robust event-triggered output feedback controllers for nonlinear systems," *Automatica*, vol. 75, pp. 96-108, 2017.

[10] M. Abdelrahim, R. Postoyan, J. Daafouz, and D. Nesic, "Stabilization of nonlinear systems using event-triggered output feedback laws," *IEEE Transactions Automatic Control*, vol. 61, no. 9, pp. 2682-2687, Sep. 2016.

[11] W. Heemels, M. Donkers, and A. Teel, "Periodic Event-Triggered Control for Linear Systems," *IEEE Transactions Automatic Control*, vol. 58, pp. 847-861, 2013.

[12] D.P. Borgers, R. Postoyan , A. Anta, P. Tabuada, D. Nesic, W.P.M.H. Heemels, "Periodic event-triggered control of nonlinear systems using overapproximation techniques," *Automatica*, vol. 94, pp. 81-87, 2018.

[13] W. Wang, R. Postoyan, D. Nesic and W.P.M.H. Heemels, "Stabilization of nonlinear systems using state-feedback periodic event-triggered controllers," in *Proceedings of the 55th IEEE Conference on Decision and Control*, Las Vegas, NV, USA, 2016, pp. 6808-6813.

[14] W. Wang, R. Postoyan, D. Nesic and W.P.M.H. Heemels, "Periodic event-triggered control for nonlinear networked control systems," *IEEE Transactions on Automatic Control*, vol. 65, pp. 620-635, 2018.

[15] W. Wang, R. Postoyan, D. Nesic and W.P.M.H. Heemels, "Periodic event-triggered output feedback control of nonlinear systems," in *Proceedings of the 57th IEEE Conference on Decision and Control*, Florida, USA, 2018, pp. 957-962.

[16] M. Fu and L. Xie, "The sector bound approach to quantized feedback control," *IEEE Transactions on Automatic Control*, vol. 50, pp. 1698-1711, 2005.

[17] R. W. Brockett and D. Liberzon, "Quantized feedback stabilization of linear systems," *IEEE Transactions on Automatic Control*, vol. 45, pp. 1279-1289, 2000.

[18] P. Tallapragada and J. Cortes, "Event-triggered stabilization of linear systems under bounded bit rates," *IEEE Transactions on Automatic Control*, vol. 61, pp. 1575-1589, 2016.

[19] A. Tanwani, C. Prieur, and M. Fiacchini, "Observer-based feedback stabilization of linear systems with event-triggered sampling and dynamic quantization," *Systems and Control Letters*, vol. 94, pp. 46-56, 2016.

[20] M. Abdelrahim, V. S. Dolk and W. P. M. H. Heemels, "Event-triggered quantized control for input-to-state stabilization of linear systems with distributed output sensors", *IEEE Transactions on Automatic Control*, vol. 64, no. 12, pp. 4952-4967, Dec. 2019.

[21] D. Liberzon, "Hybrid feedback stabilization of systems with quantized signals," *Automatica*, vol. 39, no. 9, pp. 1543-1554, 2003.

[22] T. Liu and Z. P. Jiang, "Event-Triggered Control of Nonlinear Systems with State Quantization," *IEEE Transactions on Automatic Control*, vol. 64, no. 2, pp. 797-803, Feb. 2019.

[23] Anqi Fu, Manuel Mazo Jr., "Decentralized periodic event-triggered control with quantization and asynchronous communication," *Automatica*, vol. 94, pp. 294-299, 2018.

[24] T. Liu and Z. P. Jiang, Quantized event-based control of nonlinear systems, in *Proceedings of the 54th IEEE Conference on Decision and Control*, 2015, pp. 4806-4811.

[25] E. Garcia and P. J. Antsaklis, "Model-based event-triggered control for systems with quantization and time-varying network delays," *IEEE Transactions on Automatic Control*, vol. 58, pp. 422-434, 2013.

[26] A. R. Teel and D. Nesic, "Lyapunov functions for L2 and input-to-state stability in a class of quantized control systems," in *Proc. 50th IEEE Conf. Decis. Control Eur. Control Conf.*, Orlando, FL, USA, 2011, pp. 4542-4547.

[27] D. Nesic, A. R. Teel and D. Carnevale, "Explicit computation of the sampling period in emulation of controllers for nonlinear sampled-data systems," *IEEE Transactions on Automatic Control*, vol. 54, no. 3, pp. 619-624, March 2009.

[28] R. Goebel, R. Sanfelice, and A. Teel, Hybrid dynamical systems: Modeling, Stability, and Robustness. Princeton University Press, 2012.

[29] D. Carnevale, A.R. Teel, and D. Nesic, "A Lyapunov proof of an improved maximum allowable transfer interval for networked control systems," *IEEE Transactions on Automatic Control*, vol. 52, no. 5, pp. 892-897, 2007.